

Early-onset Alzheimer disease clinical variants

Multivariate analyses of cortical thickness

Gerard R. Ridgway, PhD*
Manja Lehmann, PhD*
Josephine Barnes, PhD
Jonathan D. Rohrer,
MRCP, PhD
Jason D. Warren, PhD,
FRACP
Sebastian J. Crutch, PhD
Nick C. Fox, MD, FRCP

Correspondence & reprint
requests to Dr. Ridgway:
gerard.ridgway@ucl.ac.uk

ABSTRACT

Objective: To assess patterns of reduced cortical thickness in different clinically defined variants of early-onset Alzheimer disease (AD) and to explore the hypothesis that these variants span a phenotypic continuum rather than represent distinct subtypes.

Methods: The case-control study included 25 patients with posterior cortical atrophy (PCA), 15 patients with logopenic progressive aphasia (LPA), and 14 patients with early-onset typical amnesic AD (tAD), as well as 30 healthy control subjects. Cortical thickness was measured using FreeSurfer, and differences and commonalities in patterns of reduced cortical thickness were assessed between patient groups and controls. Given the difficulty of using mass-univariate statistics to test ideas of continuous variation, we use multivariate machine learning algorithms to visualize the spectrum of subjects and to assess separation of patient groups from control subjects and from each other.

Results: Although each patient group showed disease-specific reductions in cortical thickness compared with control subjects, common areas of cortical thinning were identified, mainly involving temporoparietal regions. Multivariate analyses permitted clear separation between control subjects and patients and moderate separation between patients with PCA and LPA, while patients with tAD were distributed along a continuum between these extremes. Significant classification performance could nevertheless be obtained when every pair of patient groups was compared directly.

Conclusions: Analyses of cortical thickness patterns support the hypothesis that different clinical presentations of AD represent points in a phenotypic spectrum of neuroanatomical variation. Machine learning shows promise for syndrome separation and for identifying common anatomic patterns across syndromes that may signify a common pathology, both aspects of interest for treatment trials. *Neurology*® 2012;79:80-84

GLOSSARY

AAO = age at onset; **AD** = Alzheimer disease; **LPA** = logopenic progressive aphasia; **MDS** = multidimensional scaling; **PCA** = posterior cortical atrophy; **SVM** = support vector machine; **tAD** = typical amnesic Alzheimer disease; **t-SNE** = t-distributed stochastic neighbor embedding; **VBM** = voxel-based morphometry.

Alzheimer disease (AD) typically presents with an insidious onset of memory impairment progressing to involve multiple cognitive domains. However, studies are increasingly stressing the importance of atypical AD variants in which memory is not the primary deficit. Some patients with AD pathology present with visuospatial and visuo-perceptual problems and are diagnosed with posterior cortical atrophy (PCA)¹; others predominantly present with language difficulties, many of whom are diagnosed with logopenic progressive aphasia (LPA).²

Previous work using voxel-based morphometry (VBM) reported common areas of gray matter reduction in PCA, LPA, and early-onset AD, particularly involving temporoparietal regions, pointing toward a spectrum of phenotypes in AD.³ Here, we study cortical thickness (a simpler measure to interpret) in patients with early-onset typical amnesic AD (tAD), PCA,

*These authors contributed equally to this work.

From the Dementia Research Centre (G.R.R., M.L., J.B., J.D.R., J.D.W., N.C.F.) and Wellcome Trust Centre for Neuroimaging (G.R.R.), UCL Institute of Neurology, University College London, London, UK.

Study funding: Funding information is provided at the end of the article.

Go to Neurology.org for full disclosures. Disclosures deemed relevant by the authors, if any, are provided at the end of this article.

and LPA, assessing differences and commonalities in cortical thickness patterns for different clinical presentations. We then use multivariate machine learning algorithms to assess clustering and separation of patients from control subjects and of syndromes from each other.

METHODS Subjects. We studied 25 patients with PCA (age [mean \pm SD] 62.2 \pm 7.2 years, 56% male, age at symptom onset [AAO] 58.2 \pm 6.6 years), 15 patients with LPA (age 60.4 \pm 6.1 years, 67% male, AAO 56.3 \pm 5.3 years), 14 patients with tAD (age 60.8 \pm 5.2 years, 43% male, AAO 56.3 \pm 3.9 years), and 30 healthy control subjects (age 63.9 \pm 6.7 years, 50% male). Of the patients, 6 with PCA (24%), 9 with LPA (60%), and 5 with tAD (36%) had postmortem confirmed AD pathology. Groups did not differ significantly in age, gender, or AAO, although control subjects were slightly older than subjects with tAD ($p = 0.05$). A subset of 29 genotyped patients showed no significant disease by *APOE* status association ($p > 0.17$). All patients fulfilled the respective clinical criteria.^{2,4,5}

Standard protocol approvals, registrations, and patient consents. All clinically affected subjects had attended the Specialist Cognitive Disorders Clinic at the National Hospital for Neurology and Neurosurgery, London, UK. Informed consent was obtained from all subjects, and the study had local ethics committee approval.

Imaging. T1-weighted volumetric MRI scans (124 contiguous 1.5-mm coronal slices) were acquired using an inversion recovery spoiled gradient recalled sequence on 3 identical 1.5-T General Electric Signa units (no significant group by scanner association, $p > 0.25$). FreeSurfer 4.5.0⁶ was used to extract and align the cortical surfaces, resulting in thickness measurements at approximately 300,000 points (vertices) on an average surface, which were smoothed to 20-mm full-width at half-maximum. Vertices in FreeSurfer's medial wall region were excluded from subsequent analysis. Two modifications to standard FreeSurfer processing were undertaken: a locally generated brain mask was used, and FreeSurfer ventricular segmentations were added to its white matter mask to improve segmentation.

Statistics. Regional cortical thickness variations were assessed with a vertex-wise general linear model using SurfStat (<http://www.nitrc.org/projects/surfstat>). Cortical thickness was modeled as a function of group, controlling for age, gender, and scanner. Two-tailed t contrasts were thresholded to control familywise error at $p < 0.05$. Intersection maps were produced, highlighting common atrophy in the patient groups (the conjunction of the 3 syndrome vs control contrasts).

Multivariate machine learning. Considering each subject's cortical thickness measurements simultaneously at every vertex yields high-dimensional multivariate patterns. To visualize the distribution of subjects based on these cortical thickness profiles, we use multidimensional scaling (MDS) and a sophisticated nonlinear technique called t -distributed stochastic neighbor embedding (t-SNE).⁷ Both MDS and t-SNE are data-driven or unsupervised methods (i.e., trained without group information) that preserve distances between pairs of subjects to reveal neighborhood relationships and clusters. Here, the distance between 2 subjects is defined as $1 - r$, where r is the Pearson correlation

between the subjects' cortical thickness profiles — vectors of the $\sim 300,000$ thickness values (after adjustment for age, gender, and scanner using the univariate general linear model).

MDS minimizes discrepancies of intersubject distances in a 2-dimensional representation with respect to the intersubject distances in the original high-dimensional space. Although intuitively appealing, this criterion can be dominated by larger distances, neglecting the local neighborhood structure that is important for clustering. Instead of directly matching distances, t-SNE matches the high- and low-dimensional distributions of the data probabilistically: the probability of 2 points relates to their proximity such that the criterion appropriately balances shorter and longer distances. We report both MDS and t-SNE because the latter is not guaranteed to converge to the global optimum of the more complicated probabilistic criterion; broadly similar visualizations using each technique would suggest that an acceptable optimum had been found.

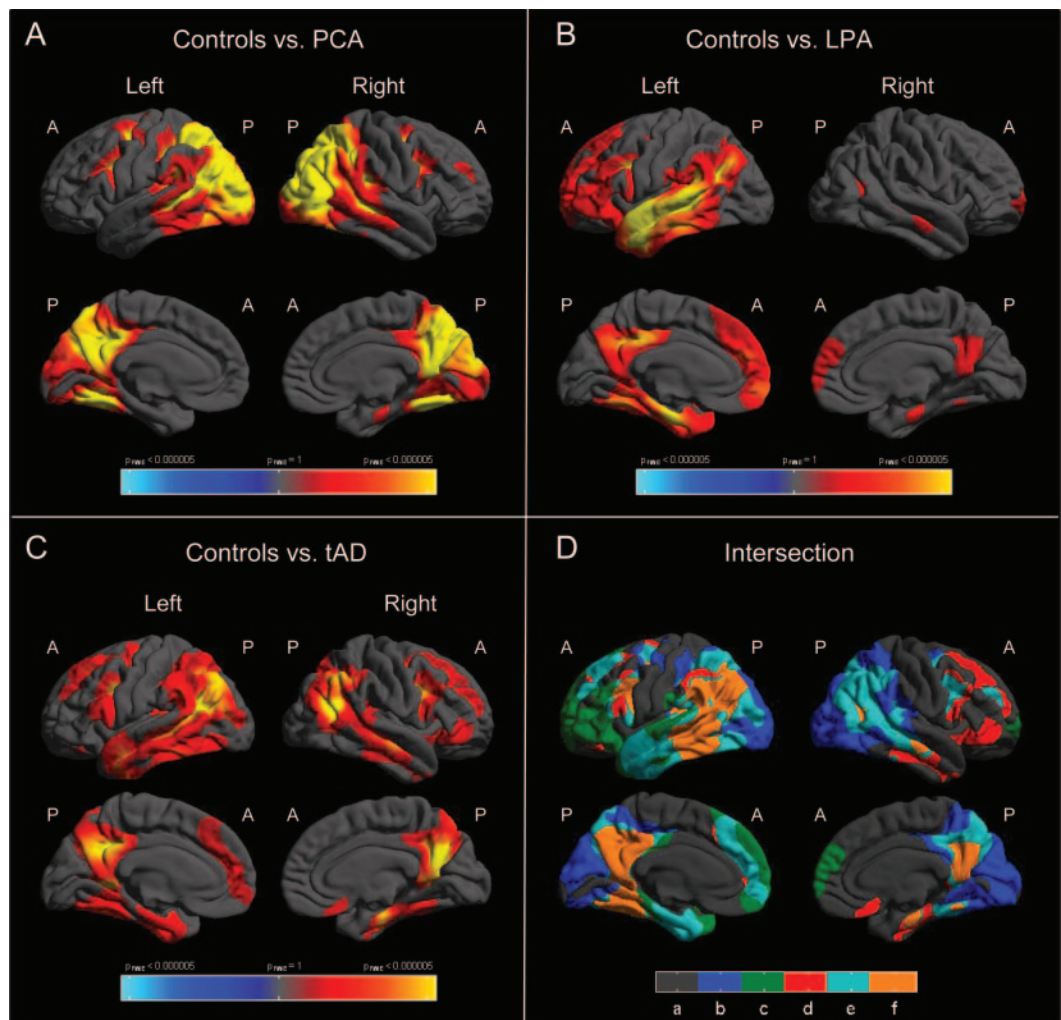
After the visualizations, we quantify group separation by using a "kernel" matrix derived from the above intersubject distances in a supervised machine learning classifier (support vector machine [SVM]).^{8,9} One classifier was trained to separate control subjects from patients (pooling all patient groups), with resultant SVM scores subsequently labeled by group. Three separate classifiers were then trained specifically to discriminate each pair of patient groups.

We used the SVM approach because of its suitability for very high-dimensional data. With high dimensionality, a particular way of separating groups determined with training data might not successfully separate unseen test data; SVMs address this by finding the dimension along which the groups are separated with the widest margin, as this typically generalizes well to new data. Here we used a soft-margin SVM, which allows some of the training data to be misclassified to obtain an even wider margin. To optimize the tradeoff between soft-margin width and misclassifications without biasing the estimated performance, a second (inner) cross-validation is needed on the training data⁸; because of the few subjects, we used a nested leave-one-out procedure to accomplish this efficiently.⁹

RESULTS Figure 1 presents regional differences in cortical thickness between the patient groups and control subjects. In PCA, cortical thickness was most significantly reduced in posterior regions including bilateral parietal and occipital areas, as well as the posterior cingulate gyrus and precuneus (figure 1A). In contrast, lower cortical thickness in subjects with LPA compared with control subjects occurred predominantly in left hemisphere temporal and frontal lobe regions (figure 1B). The most significant cortical thickness reductions in the tAD group were in bilateral temporal and posterior parietal lobe regions, as well as in the precuneus and posterior cingulate (figure 1C). The greatest overlap for the 3 patient groups (figure 1D) was found in the left hemisphere, including parietal, inferior temporal, and middle frontal lobe regions, as well as precuneus, fusiform, and posterior cingulate. Right hemisphere overlap was also found, in medial and superior temporal lobes, precuneus, fusiform, and posterior cingulate.

The visualizations in figure 2 show a notable tendency for control subjects to separate naturally from

Figure 1 Regional differences in cortical thickness between control subjects and subjects with (A) posterior cortical atrophy (PCA), (B) logopenic progressive aphasia (LPA), and (C) typical amnestic Alzheimer disease (tAD)



The color scale represents familywise error–corrected p values thresholded at 0.05. Red and yellow represent lower cortical thickness in the patient groups compared with control subjects (no regions had significantly greater cortical thickness; blue colors). (D) Intersection map showing conjunctions of reduced cortical thickness between subjects with PCA and control subjects, subjects with LPA and control subjects, and subjects with tAD and control subjects: (a) no reductions in cortical thickness; (b) reduced in PCA only; (c) reduced in LPA only; (d) reduced in tAD only; (e), reduced in any 2 patient groups; (f) reduced in all 3 patient groups, each compared with control subjects. A = anterior; P = posterior.

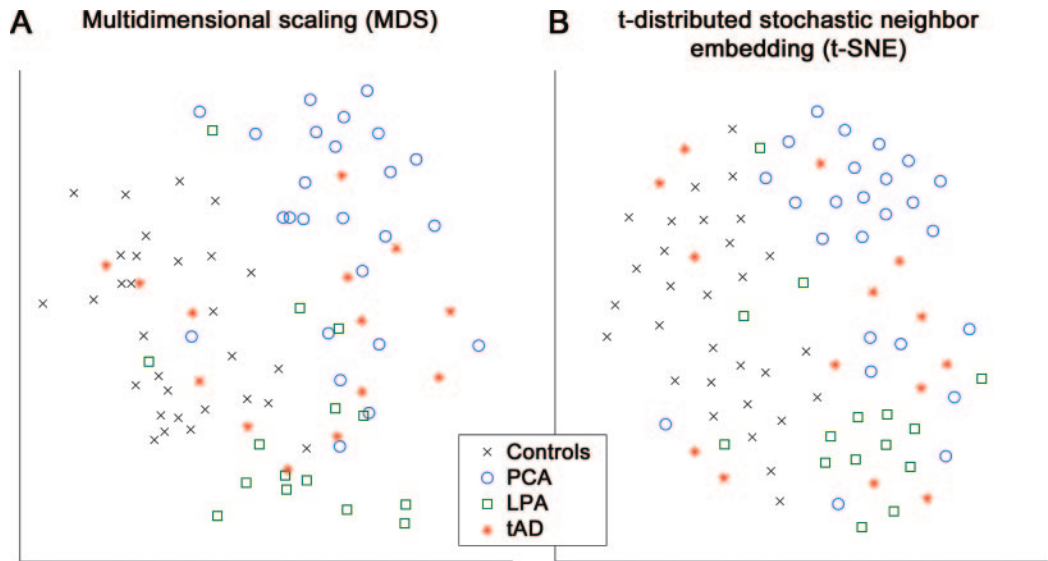
patients, but for patient groups to be more interspersed. Results from MDS and t -SNE are qualitatively similar, but the more sophisticated method achieves better clustering. Among patient groups, the subjects with PCA and LPA are best separated and the subjects with tAD are distributed along a spectrum between these extremes (with several straying into the territory of the control subjects).

Quantitative results from SVM classification analyses were consistent with the visualizations. Control subjects separated well from all patients, although no natural separation emerged among patient groups (figure 3A). However, separate classifiers trained directly to distinguish pairs of patient groups

achieved significant discrimination for every pair (figure 3B), again best distinguishing PCA and LPA.

DISCUSSION Patterns of cortical thickness in different clinical variants of AD were assessed. Common regions of lower cortical thickness in patients with PCA, LPA, and tAD compared with control subjects included predominantly left hemisphere temporoparietal areas. These findings are in accordance with the data reported for VBM³; however, there was less involvement of the right hemisphere in our study because of predominant atrophy in the left hemisphere in the LPA group. The overlapping regions found to be affected in the 3 AD variants in

Figure 2 Two-dimensional visualizations of the distribution of subjects in terms of their high-dimensional cortical thickness profiles

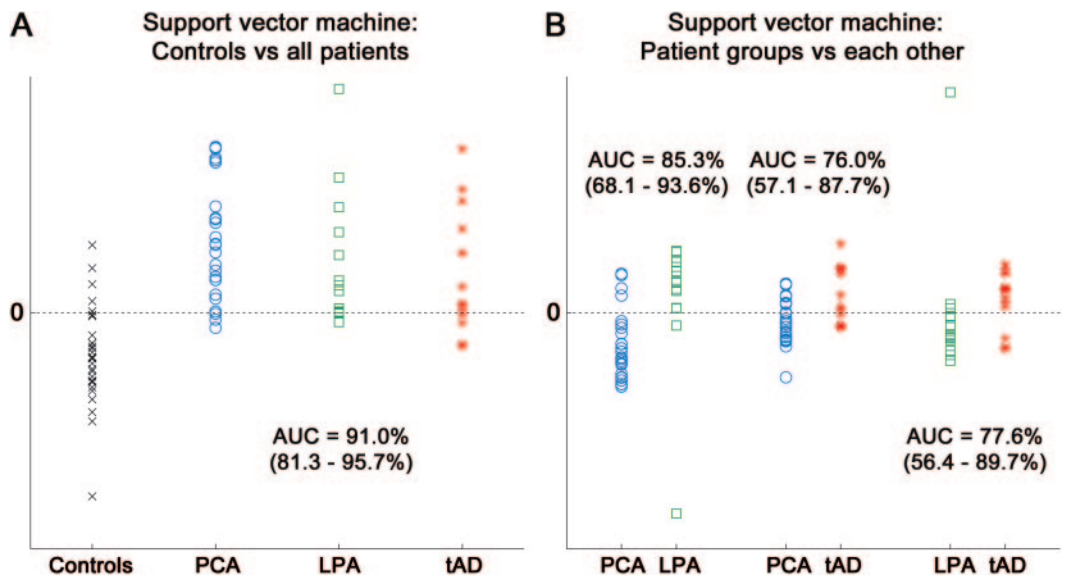


(A) Multidimensional scaling (MDS), which tries to represent the distances between subjects' multivariate cortical thickness profiles from the high-dimensional space as accurately as possible in the low-dimensional visualization, in terms of minimum squared distance error. (B) t-distributed stochastic neighbor embedding (t-SNE), which optimizes a nonlinear function of the distances to better balance the representation of the overall structure of the data with the local neighborhood structure of clusters. Axes are arbitrary and have been rotated for visual agreement between MDS and t-SNE. LPA = logopenic progressive aphasia; PCA = posterior cortical atrophy; tAD = typical amnesic Alzheimer disease.

this study have been shown to be preferentially affected by pathologic, structural, and functional changes in AD⁹ and closely match regions commonly associated with the default mode network.¹⁰ Al-

though common areas were found in these 3 variants, differences were also suggested, with the control comparisons showing different atrophy patterns in each patient group, involving regions typically associ-

Figure 3 Supervised support vector machine (SVM) classification of control subjects and patients and of AD variant groups



(A) SVM trained to separate all 54 patients from control subjects, with patients subsequently relabeled into their separate groups. (B) Results from 3 separate SVM analyses, each trained to separate 1 patient group from another patient group. All SVMs used a kernel matrix derived from the distance matrix used in figure 2. Performance of each SVM is summarized by the area under the curve (AUC) of the receiver operating characteristic, with 95% confidence intervals in parentheses. LPA = logopenic progressive aphasia; PCA = posterior cortical atrophy; tAD = typical amnesic Alzheimer disease.

ated with these syndromes, i.e., bilateral occipital and parietal lobe regions in PCA, left temporoparietal and superior temporal lobe regions in LPA, and bilateral medial temporal and posterior parietal regions in tAD.

Previous work showed group-specific areas of atrophy only without correction for multiple comparisons.³ Here, the multivariate SVM analyses reveal that significant separation is possible between every pair of patient groups (confidence interval lower limits greater than the 50% chance level). However, consistent with the continuum hypothesis,³ and perhaps unsurprisingly, the patient groups are less well separated from each other than they are as a whole from control subjects, both in the SVM and the unsupervised dimensionality reduction visualizations. The latter show a tendency for tAD to be distributed among the relatively more distinct clusters formed by the other 2 patient groups and control subjects, but even the best separated LPA and PCA groups exhibit some degree of overlap consistent with the hypothesis of a spectrum of variation as opposed to distinct groups. Machine learning may be useful for identifying common anatomic patterns across different clinical syndromes that may signify common pathology. Identification of common anatomic patterns may signify a homogeneous target pathophysiology that could be the subject of clinical trials or biomarker studies.

STUDY FUNDING

This work was undertaken at UCLH/UCL, which received a proportion of funding from the Department of Health NIHR Biomedical Research Centres funding scheme. The Dementia Research Centre is an Alzheimer's Research UK Co-ordinating Centre and has also received equipment funded by Alzheimer's Research UK. The Wellcome Trust Centre for Neuroimaging is supported by core funding from the Wellcome Trust (079866/Z/06/Z). Some of the data used here come from the MIRIAD study, which was funded by the Alzheimer's Society. M.L. is supported by the Alzheimer's Society. J.D.W. is supported by a Wellcome Trust Senior Clinical Fellowship. S.C. is supported by an Alzheimer's Research UK Senior Research Fellowship. N.C.F. is supported by an MRC (UK) Senior Clinical Fellowship and holds a National Institute for Health Research (NIHR) senior investigator award.

AUTHOR CONTRIBUTIONS

Dr. Ridgway: analysis or interpretation of data; drafting/revising manuscript for content; statistical analysis. Dr. Lehmann: analysis or interpretation of data; drafting/revising manuscript for content. Dr. Barnes: drafting/revising manuscript for content. Dr. Rohrer: drafting/revising manuscript for content. Dr. Warren: drafting/revising manuscript for

content; study concept or design. Dr. Crutch: drafting/revising manuscript for content; study concept or design. Prof. Fox: drafting/revising manuscript for content; study concept or design.

ACKNOWLEDGMENT

G.R. thanks Dr. Tom Diethe, Honorary Research Associate at UCL Department of Computing, for first introducing him to the t-SNE method. The authors thank Dr. Jonathan Schott, Senior Lecturer and Honorary Consultant Neurologist at the Dementia Research Centre, for providing subjects from the MIRIAD dataset, Drs. Matthew Clarkson and Sébastien Ourselin at the UCL Centre for Medical Image Computing for the development of software pipelines, and all the patients and their families who took part in this research.

DISCLOSURE

G.R. Ridgway serves as an editorial board member for *NeuroImage* and has received honoraria for teaching on SPM courses. M. Lehmann, J. Barnes, J.D. Rohrer, J.D. Warren, and S.J. Crutch report no disclosures. University College London has received payment from Abbott, Eisai, Elan, Eli Lilly, GE Healthcare, IXICO, Janssen, Lundbeck, Pfizer, sanofi-aventis, and Wyeth Pharmaceuticals for image analysis services and/or for consultancy by N.C. Fox. **Go to Neurology.org for full disclosures.**

Received October 28, 2011. Accepted in final form February 23, 2012.

REFERENCES

1. Benson F, Davis J, Snyder BD. Posterior cortical atrophy. *Arch Neurol* 1988;45:789–793.
2. Gorno-Tempini ML, Hillis AE, Weintraub S, et al. Classification of primary progressive aphasia and its variants. *Neurology* 2011;76:1006–1014.
3. Migliaccio R, Agosta F, Rascovsky K, et al. Clinical syndromes associated with posterior atrophy early age at onset AD spectrum. *Neurology* 2009;73:1571–1578.
4. Dubois B, Feldman HH, Jacova C, et al. Research criteria for the diagnosis of Alzheimer's disease: revising the NINCDS-ADRDA criteria. *Lancet Neurol* 2007;6:734–746.
5. Tang-Wai DF, Graff-Radford NR, Boeve BF, et al. Clinical, genetic, and neuropathologic characteristics of posterior cortical atrophy. *Neurology* 2004;63:1168–1174.
6. Fischl B, Sereno MI, Dale AM. Cortical surface-based analysis: II: inflation, flattening, and a surface-based coordinate system. *Neuroimage* 1999;9:195–207.
7. Van der Maaten L, Hinton G. Visualizing data using t-SNE. *J Mach Learn Res* 2008;9:2579–2605.
8. Wilson SM, Ogar JM, Laluz V, et al. Automated MRI-based classification of primary progressive aphasia variants. *Neuroimage* 2009;47:1558–1567.
9. Lehmann M, Rohrer JD, Clarkson MJ, et al. Reduced cortical thickness in the posterior cingulate gyrus is characteristic of both typical and atypical Alzheimer's disease. *J Alzheimers Dis* 2010;20:587–598.
10. Buckner RL, Andrews-Hanna JR, Schacter DL. The brain's default network: anatomy, function, and relevance to disease. *Ann NY Acad Sci* 2008;1124:1–38.